AFRL-AFOSR-VA-TR-2020-0196

Studying Ultrafast Electron Dynamics in Condensed Matter with Next Gen

Zenghu Chang
UNIVERSITY OF CENTRAL FLORIDA

08/12/2020
Final Report

Air Force Research Laboratory
AF Office Of Scientific Research (AFOSR)/ RTB1
Arlington, Virginia 22203
Air Force Materiel Command

DISTRIBUTION A: Distribution approved for public release.

REPORT DOCUMENTATION PAGE

Form Approved
OMB No. 0704-0188

1. REPORT DATE *(DD-MM-YYYY)*	2. REPORT TYPE	3. DATES COVERED *(From - To)*
16-10-2020	Final Performance	15 Dec 2014 to 14 Jun 2020

4. TITLE AND SUBTITLE
Studying Ultrafast Electron Dynamics in Condensed Matter with Next Gen

5a. CONTRACT NUMBER

5b. GRANT NUMBER
FA9550-15-1-0037

5c. PROGRAM ELEMENT NUMBER
61102F

6. AUTHOR(S)
Zenghu Chang, Daniel Neumark, Louis DiMauro, Mark Stockman, Pierre Agostini, Stephen Leone

5d. PROJECT NUMBER

5e. TASK NUMBER

5f. WORK UNIT NUMBER

7. PERFORMING ORGANIZATION NAME(S) AND ADDRESS(ES)
UNIVERSITY OF CENTRAL FLORIDA
4000 CNTRL FLORIDA BLVD
ORLANDO, FL 32816 US

8. PERFORMING ORGANIZATION REPORT NUMBER

9. SPONSORING/MONITORING AGENCY NAME(S) AND ADDRESS(ES)
AF Office of Scientific Research
875 N. Randolph St. Room 3112
Arlington, VA 22203

10. SPONSOR/MONITOR'S ACRONYM(S)
AFRL/AFOSR RTB1

11. SPONSOR/MONITOR'S REPORT NUMBER(S)
AFRL-AFOSR-VA-TR-2020-0196

12. DISTRIBUTION/AVAILABILITY STATEMENT
A DISTRIBUTION UNLIMITED: PB Public Release

13. SUPPLEMENTARY NOTES

14. ABSTRACT
The first generation attosecond light sources were driven by few-cycle near-infrared Ti :Sapphire lasers centered at 800 nm. The photon energy of the generated single isolated attosecond pulses are limited to 150 eV. The MURI team demonstrated isolated 53-as pulses with continuous spectra extending to the water window spectral region. The extremely broad bandwidth covers the carbon K-edge and the boron K-edge. The breakthrough was achieved by using a 3 mJ, two-cycle, 1 kHz, carrierenvelope phase-stable laser source at 1.7 m. A novel scheme for attosecond phase retrieval from noisy streaking traces was developed, which is based on conditional variational generative network. It has the ability to incorporate a complete physics model of the streaking process, and the ability to model the uncertainty of pulse reconstruction in the presence of noise. In-situ methods were introduced as an efficient, all-optical approach to attosecond pulse measurement in which measurement and pulse generation take place simultaneously. While the next generation attosecond light sources are being developed, new physics experiments using the Ti :Sapphire based first generation sources have obtained exciting results with solid and water jet targets. A new powerful tool, attosecond transient reflectivity has been demonstrated. Both attosecond transient absorption and attosecond transient reflectivity have been successfully used in investigating the dynamics of core-level excitons in semiconductors and insulators, carrier thermalization and coherent phonon dynamics in metals, as well as coherent magnetism in multi-layer systems. In addition, theoretical study of attosecond optical field control of electron population and symmetry in a two dimensional material silicone, graphene and transition metal dichalcogenides has suggested new schemes to measure fundamental topological properties.

15. SUBJECT TERMS
attosecond, high harmonic generation, x-ray, ultrafast, electron dynamics

16. SECURITY CLASSIFICATION OF:			17. LIMITATION OF ABSTRACT	18. NUMBER OF PAGES	19a. NAME OF RESPONSIBLE PERSON
a. REPORT	b. ABSTRACT	c. THIS PAGE			STICKRATH, ANDREW
Unclassified	Unclassified	Unclassified	UU		19b. TELEPHONE NUMBER *(Include area code)* 703-696-9511

FA9550-15-1-0037: Studying Ultrafast Electron Dynamics in Condensed Matter with Next Generation Attosecond X-ray Sources

Final report

August 12, 2020

Zenghu Chang (lead PI), University of Central Florida
Pierre Agostini, Ohio State University
Louis F. DiMauro, Ohio State University
Stephen R. Leone, University of California, Berkeley
Daniel M. Neumark, University of California, Berkeley
Mark I. Stockman, Georgia State University
Paul B. Corkum, University of Ottawa, Canada
Ferenc Krausz, Ludwig Maximilian University of Munich, Germany

Abstract

The first generation attosecond light sources were driven by few-cycle near-infrared (NIR) Ti:Sapphire lasers centered at 800 nm. The photon energy of the generated single isolated attosecond pulses (IAPs) are limited to 150 eV. The MURI team demonstrated isolated 53-as pulses with continuous spectra extending to the water window spectral region. The extremely broad bandwidth covers the carbon K-edge and the boron K-edge. The breakthrough was achieved by using a 3 mJ, two-cycle, 1 kHz, carrier-envelope phase-stable laser source at 1.7 μm. A novel scheme for attosecond phase retrieval from noisy streaking traces was developed, which is based on conditional variational generative network. It has the ability to incorporate a complete physics model of the streaking process, and the ability to model the uncertainty of pulse reconstruction in the presence of noise. In-situ methods were introduced as an efficient, all-optical approach to attosecond pulse measurement in which measurement and pulse generation take place simultaneously. While the next generation attosecond light sources are being developed, new physics experiments using the Ti:Sapphire based first generation sources have obtained exciting results with solid and water jet targets. A new powerful tool, attosecond transient reflectivity has been demonstrated. Both attosecond transient absorption and attosecond transient reflectivity have been successfully used in investigating the dynamics of core-level excitons in semiconductors and insulators, carrier thermalization and coherent phonon dynamics in metals, as well as coherent magnetism in multi-layer systems. In addition, theoretical study of attosecond optical field control of electron population and symmetry in a two dimensional material silicone, graphene and transition metal dichalcogenides has suggested new schemes to measure fundamental topological properties.

1.Scientific Progress and Accomplishments

1.1 Next Generation Attosecond Light Sources

1.1.1 Attosecond pulse retrieval from noisy streaking traces with conditional variational generative network, Chang

Compared to its femtosecond laser characterization with FROG (Frequency Resolved Optical Gating), attosecond phase retrieval suffers from both experimental and theoretical challenges. The photon flux of attosecond soft X-ray is much lower than that in a typical FROG experiment, giving rise to higher statistic noise in the streaking trace. Accurate characterization of an attosecond pulse

from broadband streaking trace in the water window is an indispensable step in studying the ultrafast electron dynamics on the attosecond scale. Conventional attosecond pulse retrieval methods face two major challenges: the ability to incorporate a complete physics model of the streaking process, and the ability to model the uncertainty of pulse reconstruction in the presence of noise. We developed a pulse retrieval method based on conditional variational generative network (CVGN) that can address both demands.

Instead of using a neural network to learn the direct mapping from a streaking trace to a pulse profile, the CVGN models the distribution of the pulse profile conditioned on a given streaking trace measurement, and is thus capable of assessing the uncertainty of the retrieved pulses. This capability is highly desirable for low-photon level measurement, which is typical in attosecond streaking experiments in the water window X-ray range. In addition, the proposed scheme incorporates a refined physics model that considers the Coulomb-laser coupling and photoelectron angular distribution in streaking trace generation. CVGN pulse retrievals under various simulated noise levels and experimental measurement have been demonstrated. The results showed high pulse reconstruction consistency for streaking traces when peak signal-to-noise ratio (SNR) exceeds 6, which could serve as a reference for future learning-based attosecond pulse retrieval.

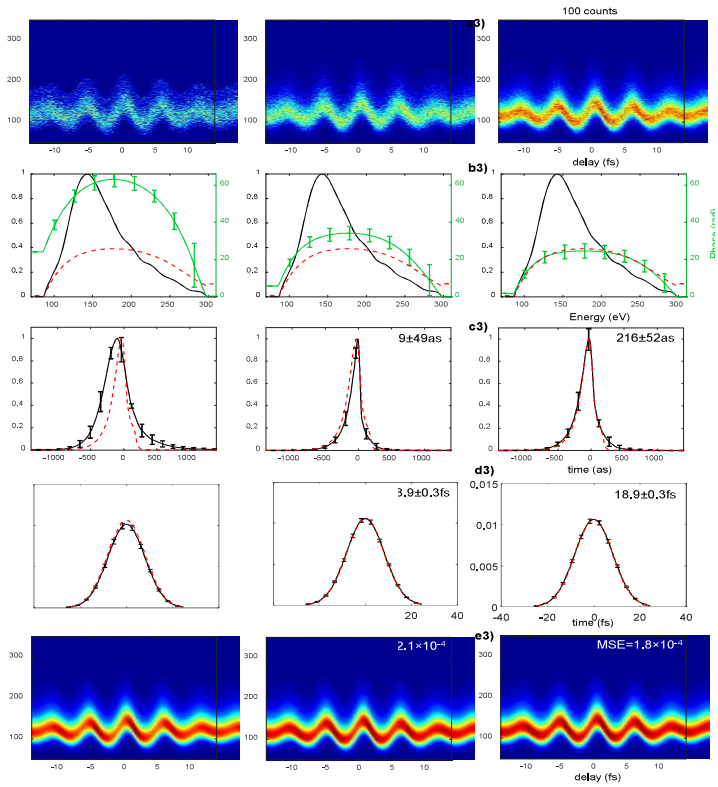

Fig.1. Pulse retrieval from a simulated streaking trace. (a) Input streaking traces. (b, c) Retrieved X-ray spectral phase (b) and temporal envelop (c). (d) Reconstructed IR pulse in time domain. The dashed red curves on (b-d) indicate the ground truth. Error bars on (b-d) represent the variance of the retrieved pulse instances. Numbers on the upper right corner indicate FWHM of retrieved pulse. (e) Reconstructed streaking trace from the retrieved pulses. The MSE indicates the error between the reconstructed streaking trace and the ground truth.

The training data were generated by adding noise to the ideal, noise-free traces from the physics model. We first created 10000 ideal traces with random pulse parameters, $\mathbf{x}$, and normalized their intensities to the range between 0 and 1. Poisson noise was added to each ideal trace $\mathbf{y}_0$ to simulate noisy traces in experiments

$$\mathbf{y} \sim Poisson(\lambda \mathbf{y}_0), \qquad (1)$$

where the parameter λ is the average peak count of the Poisson distribution.

Fig. 1 (a1-a3) shows three simulated streaking traces from the same noise-free test trace with λ=5, 21 and 100. For each trace, 25 instances of the pulse parameter set, $\hat{\mathbf{x}}$, were retrieved from the posterior distribution $p_\gamma(\mathbf{x}|\mathbf{y},\mathbf{z})$. The frequency (Fig. 1 (b1-b3)) and time-domain (Fig. 1 (c1-c3)) X-ray pulses, along with the time-domain envelop of IR pulses (Fig. 1 (d1-d3)), were reconstructed from these retrieved pulse parameters. Streaking traces (Fig. 1 (e1-e3)) were then generated from the retrieved X-ray and IR pulses using the physical model in Eq. (1)-(4). Error bars on Fig. 1 (b-d) represent the variance of the 25 instances of retrieved X-ray pulse.

The reconstructed streaking traces and the full-width-at-half-maximum (FWHM) of the time-domain X-ray pulse were compared with the ground truth. The mean squared error (MSE) of the 25 reconstruction instances was used as the error metric to evaluate the performance under various noise levels. The reconstructed and ideal streaking traces were all normalized to facilitate the comparison among various λ. For the errors on pulse duration, the MSE was normalized by the FWHM of the X-ray ground truth, which was 209 as in the simulation.

The results show that as the average peak count, λ, exceeds 32.5, the MSE of the reconstructed streaking trace decreased and remained below 3.5×10^{-4}. The MSE of pulse duration also decreased from ~80% (λ=5) down to 6% (λ=32.5). The results suggest an average peak Poisson SNR of at least 6 to achieve satisfactory pulse retrieval. It is worth noting that for low photon count (5 counts), the retrieved X-ray field exhibits increased bias in pulse profile, which is an indication of strong regularization. This is the effect of using the training data with mixed noise level, which can be reduced by training with traces with same noise level or implementing additional mechanism to adjust the posterior distribution based on noise level. The retrieved time-domain IR envelop, on the other hand, is less affected by the noise. This is because IR envelop is represented by a Gaussian function with relatively few parameters, and is oversampled by 20 delays per cycle in the streaking measurements. Because of CVGN's flexibility in capturing the distribution of solutions satisfying a physical model, it is not necessary to restrict the IR envelop to a Gaussian shape. We envision a complex IR envelop (amplitude and phase chirp) can be retrieved by using more parameters describing the IR field.

1.1.2 Waveform synthesis for attosecond metrology, Krausz

Using CEP stable few-cycle pulses generated from the OPA system at MPQ with 2.1 μm central wavelength, on which was reported previously, a supercontinuum was generated within an air-filled hollow core fiber that extended from 300 nm to around 3 μm (figure). The simplified two-stage OPA design has over the last couple years provided a superior day-to-day reproducibility, as depicted by the average and standard deviation of the OPA output spectrum (figure, top left). The supercontinuum was divided into three channels, to facilitate dispersion compensation using chipped mirrors and wedges. The high frequency channel of the synthesizer (shown in blue, figure) was designed specifically with waveform metrology in mind. With the design and subsequent implementation of proper dispersion compensation, the "blue" channel, with a power of 160 μW, provided the necessary probe field for performing electro-optic sampling (EOS) of the waveform transients synthesized using the other two channels, successfully extending the range of EOS to red side of the visible spectral range (700 nm). As compared to attosecond streaking, field metrology using EOS is based on non-linear optics, does not require a vacuum infrastructure, and has been shown to have advantages in terms of sensitivity and dynamics range.

By adjusting the relative delay between the two IR channels, the field of the synthesized transients could be adjusted—providing the means for directly tuning the electric field and producing transients of sub-cycle duration. With irises used to throttle the pulse energy of the two IR channels during synthesis, the pulse energy of the <4 fs transients was around 1.6 μJ and thus the peak power of 400 MW should be sufficient for our future attosecond experiments.

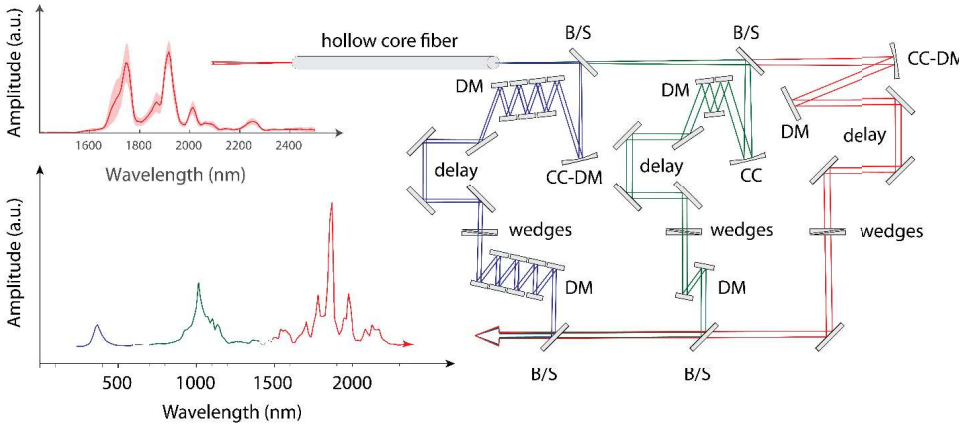

Fig. 2. A waveform synthesizer for ultrafast metrology with a high frequency (VIS-UV) channel for direct EOS characterization of the electric field of the transients produced by synthesizing the two IR channels.

1.2 Attosecond experimental end-station and two-source transient absorption spectroscopy, Agostini and DiMauro

The OSU group had proposed the design of a new photon spectrometer capable of resolving energies up to 600 eV, as well as building a new beamline to perform preliminary attosecond transient absorption spectroscopy measurements in 2D materials. The group has designed, built and commissioned both a photon spectrometer with a spectral range of 20 – 1,240 eV and a new flexible beamline that can accommodate different end-stations. Two end-stations were specifically designed and commissioned for this project: a gas/solid sample target chamber and the aforementioned photon spectrometer.

The OSU group has performed preliminary transient absorption measurements in both gaseous and condensed matter systems. The stability of the instrument was demonstrated by measuring the sub-cycle dynamics of the Argon Fano resonance induced with a long wavelength (λ = 1255 nm) excitation; see Fig 3 (a). Preliminary transient absorption measurements of Si using a multi-photon excitation (1590 nm) reveal a previously unreported broad spectral feature centered at ~70 eV, in addition to the well-known L-edge feature at ~100 eV; see Fig. 4(b). The OSU group initiated a collaboration with material scientists Prof. S. K. Sundaram (Alfred University) and Y. Du, G. Johnston, V. Prabhakaran & L. Wang (PNNL) to obtain high quality thin membrane samples grown via MBE and a novel ambient soft landing deposition technique. This collaboration has provided high quality samples of Cr_2O_3 and $PW_{12}O_{40}$. The ground states of these materials have been measured (see Fig. 3 (c)-(d)) and the OSU group is preparing to measure the transient absorption spectra.

The polyoxometalate $PW_{12}O_{40}$ is part of a larger class of materials with a Keggin structure. Owing to their unique capacitance properties, these materials have earned the moniker "electron sponges" by absorbing up to 24 electrons without structural damage; see Fig.3 (f). The OSU group plans to study the electron dynamics following photoinjection from the membrane substrate.

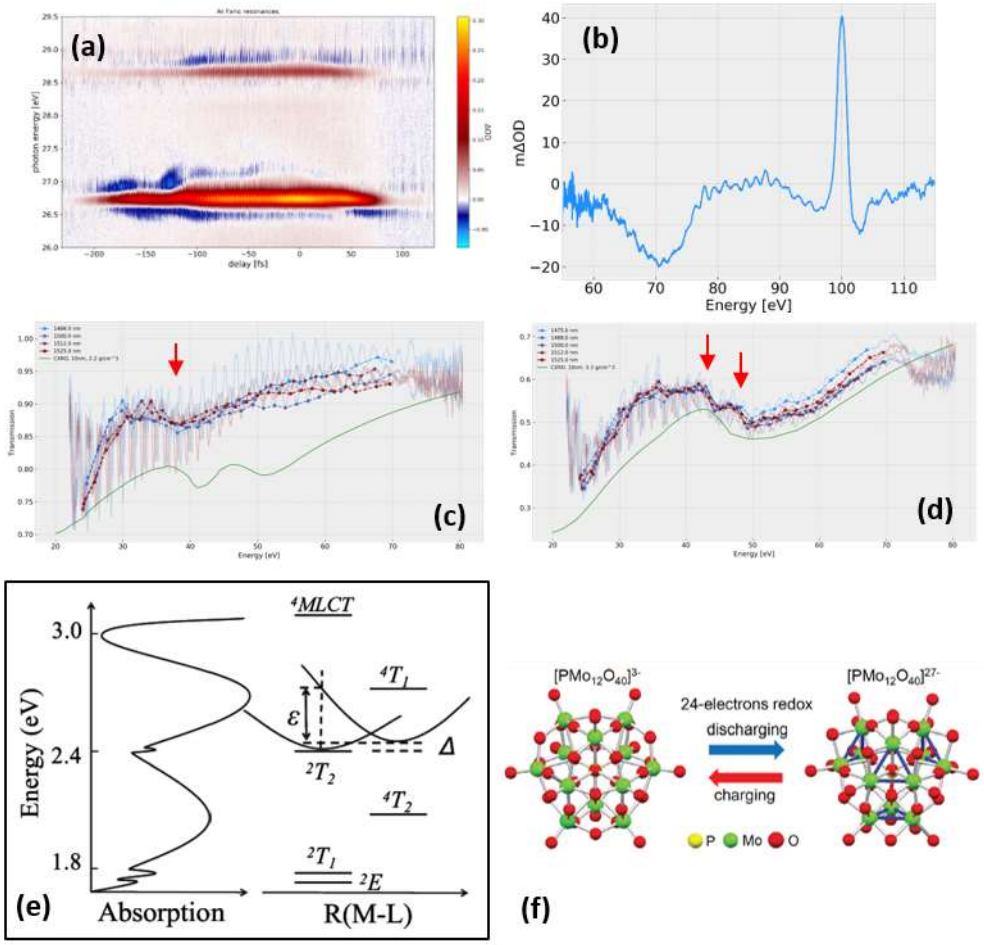

Fig. 3. (a) Argon Fano resonances excited via a long wavelength (λ = 1255 nm) excitation. Sub-cycle oscillations, representing a beating between the two Fano states, are visible at 2ω (2.09 fs). The high contrast of these oscillations indicate the interferometric stability of the apparatus. (b) Transient absorption spectrum of a 200 nm Si membrane near temporal overlap, using multi-photon excitation (λ = 1590 nm). The large positive feature corresponds to the Si L-edge; the broad negative feature at 70 eV (previously unreported) has yet to be assigned to a physical process. (c) Ground state measurement of MBE-grown Cr_2O_3 on a nitride membrane using an XUV harmonic comb. Red arrows indicate the Cr M-edge. (d) Ground state measurement of ambient soft-landed $PW_{12}O_{40}$ on a nitride membrane. The red arrow indicates the W M-edge. For (c) and (d), the ground state was finely sampled by shifting the comb (fundamental wavelength) and taking multiple spectra. For each wavelength, the faint line represents the transmission function of the harmonic comb; the bolded dots represent the transmission function evaluated at the peak of the comb. The apparent 2ω oscillations in the transmission functions are due to the poor statistics between the tines of the harmonic comb. (e) The energy diagram of Cr_2O_3 showing a possible relaxation pathway for ultrafast demagnetization. (f) Structure of $PW_{12}O_{40}$.

Cr_2O_3 is an antiferromagnet with a Néel temperature slightly above room temperature (T_N = 307 K). The optically induced ultrafast demagnetization of Cr_2O_3 has been recently studied, but the exact relaxation pathway has not been resolved experimentally. Transient absorption provides a new way to study the relaxation pathway by probing the Cr M-edge, see Fig. 3(e). The OSU group plans to observe the spin-orbit mediated relaxation pathway that has been theoretically predicted.

In another study, we used a $0-\pi$ square-wave phase grating to shape 1350 nm and 1450 nm femtosecond pulses and create two intense lobes at the focus of a lens. We show that the relative phase between these two lobes (the ±1st-orders of diffraction of the grating) is controlled very simply and precisely by shifting the position of the grating in its plane. We generate high harmonic orders from the two bright lobes and record the beating between the two emissions for each harmonic order up to the 53rd harmonic order. Our study shows that the relative phase between the two beams created by the duplicator can be controlled with 14 mrad precision. Finally, we studied the peak intensity modulations due to interference between the different diffraction orders of the grating and gave theoretical insight into the resulting modulation of the envelope of the harmonics beating. We found that all harmonic orders in the plateau region should be affected in a similar way.

1.3 Probing and controlling electron dynamics in condensed matter

1.3.1 Attosecond transient spectroscopy and time-resolved photoelectron spectroscopy on liquid jets, Leone and Neumark

Attosecond transient absorption (ATA) and attosecond transient reflectivity (ATR) measurements in the extreme ultraviolet (XUV) have been conducted at the University of California, Berkeley under the guidance of S. Leone and D. Neumark to investigate the dynamics of core-level excitons in semiconductors and insulators, carrier thermalization and coherent phonon dynamics in metals, as well as coherent magnetism in multi-layer systems. Regarding the research on core-excitons, the Leone and Neumark group measured the dynamics and lifetime of core-excitons in bulk tungsten disulfide (WS_2) at the W $N_{6,7}$ edge and $O_{2,3}$ edge with the ATA method (Fig. 4(a)). The ATA measurements on WS_2 revealed that the lifetimes of core-excitons at the W $N_{6,7}$ edge are approximately 4 fs and the lifetimes of core-excitons at the W $O_{2,3}$ edge below 3 fs.

In addition to the study of core-excitons in non-conducting materials, the Leone and Neumark group studied electron thermalization dynamics in nickel (Ni) (Fig. 4(b)) and ultrafast demagnetization dynamics in cobalt-platinum (Co/Pt) multilayer thin films. The ATA study using a 4 fs long visible-near-infrared (Vis-NIR) pulse as the heating pump pulse on Ni showed that the electron thermalization time in Ni is approximately 10 fs and a multi-temperature model can be utilized to simulate the heat exchange between the electronic, phonon, and spin thermal bath after such time scales. In the investigation of ultrafast demagnetization dynamics on Co/Pt thin films, magnetic XUV scattering is applied in lieu of the ATA technique. The transient magnetic scattering of the Co/Pt thin film after the Vis-NIR pump pulse with different polarizations with respect to the magnetization in the thin film showed that the demagnetization dynamics are influenced by both the heating of the spin bath and the induced spin current by the electric field of the pump pulse across different magnetic domains. The study of electron thermalization and demagnetization dynamics in metals should shed further light on the mechanisms for controlling magnetizations at ultrafast time scales. Moreover, a novel XUV magnetic circular dichroism (XMCD) approach was developed to directly probe the spin dynamics of the Co/Pt thin films. Using a 4-mirror XUV phase shifter, elliptically polarized radiation was obtained and used to perform element-specific XMCD

at both the Co and Pt edges, with sub 5-fs resolution. The observed spin response (Fig. 4(c)) showed that in the first few femtoseconds, minority spin carriers are injected from Pt to Co, resulting in a coherent increase (resp. decrease) of the magnetization in the Pt (resp. Co) layers. Furthermore, spin-orbit mediated spin-flips were clearly distinguished in next 10-20 fs. These observations are the first of their kind and open numerous perspectives towards dynamic and coherent manipulation of magnetism at the few-femtosecond timescale.

Furthermore, the Leone group explored exciton, phonon and carrier dynamics in a variety of metallic and semi-metallic systems. The topic of highly coupled electronic and phonon dynamics was explored in bismuth, which presents a prototypical Peierls-Jones distortion. ATR measurements at the Bi $O_{4,5}$ edge revealed that photoexcitation leads to a complex response in which the excitation of the coherent A_{1g} phonon is accompanied by oscillation of both electron and hole temperatures, in anti-phase with the atomic motion (Fig. 4(d)). Progressing towards more complex systems, bulk semiconducting transition metal dichalcogenides were then studied with the ATA method (Fig. 4(e-f)). Probing carrier dynamics in WSe_2 at the W $N_{6,7}$ edge after a 4 fs long VIS-NIR pump pulse shows a direct bandgap transition in the layered indirect bandgap semiconductor, indicating the formation of an initial exciton in the monolayers. Simultaneous observation of Se $M_{4,5}$ edge region measures an oscillatory feature with a frequency of 7.5 THz and an intervalley

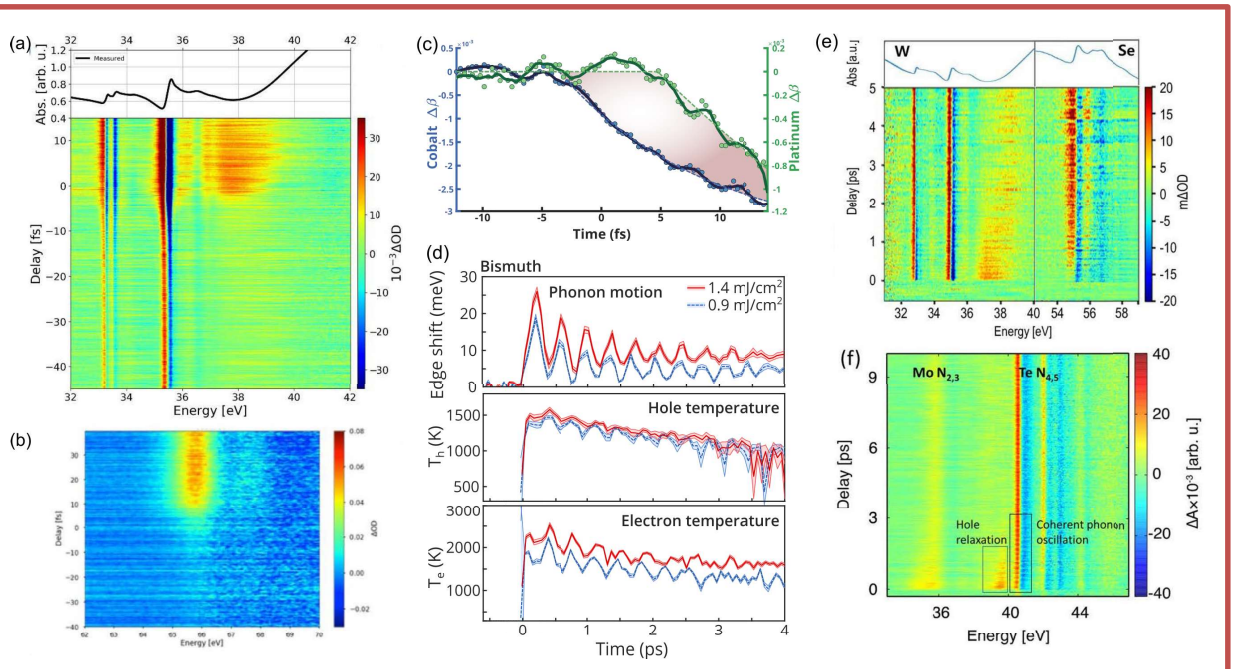

Fig. 4. (a) XUV absorption spectrum (black) of 40 nm thick WS_2 at W $N_{6,7}$ edge (32-34 eV) and $O_{2,3}$ edge (35-40 eV) and their transient absorption recorded with ATA. (b) XUV transient absorption at Ni $M_{2,3}$ edge of a 50 nm thick Ni thin film taken with ATA. (c) Attosecond magnetic circular dichroism in Co/Pt multilayers. The change in magneto-optical index is shown for Co and Pt layers (left and right axes, respectively). The shaded area highlights the different dynamics caused by coherent phenomena. (d) Bismuth photoexcited dynamics extracted from ATR measurements. The phonon motion, hole and electron temperatures are shown for two photoexcitation densities. (e) XUV absorption spectrum (top) of bulk WSe_2 at the W $N_{6,7}$ edge and Se $M_{4,5}$ edge and their transient XUV absorption feature (bottom) recorded with ATA. (f) Transient XUV absorption feature of 2H-$MoTe_2$ at Mo $N_{2,3}$ edge and Te $N_{4,5}$ edge. Hole and coherent phonon dynamics are extracted from transient absorption signal at the Te N_5 edge.

scattering time of 700 fs. This indicates that the carrier thermalization dominantly proceeds via coupling with the in-plane phonon mode, and subsequent carrier diffusion to adjacent layers is driven by intervalley scattering. Investigation into carrier dynamics of 2H-$MoTe_2$ with the same technique shows a sub-30 fs hole thermalization time and electron-hole recombination time at 1.5 ps. In addition, our results show displacive excitations of coherent A_{1g} and E_{1g} phonons (Fig. 4(f)). These unique electronic properties of layered semiconductors shed light on their superior properties into photo-energy conversion systems.

Apart from studying few-femtosecond dynamics in solids, the Neumark group also conducted experiments on the dynamics of nucleic acid constituents in liquid jets using UV pump-probe time-resolved photoelectron spectroscopy (TRPES). Thus far, there is one published paper on adenosine and adenosine monophosphate and a second paper in preparation on thymine-containing nucleic acid constituents. While this work has been ongoing, a beamline for generating femtosecond XUV pulses has been constructed, with the goal of carrying out UV/XUV TRPES on liquid jets. This beamline and its incorporation into the liquid jet experiment will be a key new focus of the laboratory in the coming months.

1.3.2 Attosecond strong-field processes in condensed matter, Stockman

Topological resonance is manifested by a selective population of a conduction band of a two-dimensional hexagonal solid (D_{3h} point group symmetry), in particular, transition metal dichalcogenides (TMDCs), gapped graphene, and hexagonal boron nitride (h-BN). This resonance is due to a constructive interference involving two phases: the dynamical phase, $\varphi_D = \Delta_g t$, where Δ_g is the bandgap and t is time and the topological (Berry) phase.

We have earlier established that graphene does not exhibit a pronounced topological resonance but the TMDCs do. The difference between these two classes of compounds is the chemical composition and symmetry (D6h for graphene vs. D_{3h} for TMDCs). The point symmetry also defines whether the material is a semimetal (D_{6h} is for the gapless graphene) or semiconductor (D_{3h} for TMDCs allows for a finite bandgap). A remaining question is whether the presence of the topological resonance is due just to the D_{3h} symmetry, or to chemical composition difference, which also leads to a significant spin-orbit coupling (SOC) in TMDCs but not in graphene.

We have answered that question. We have shown that the topological resonance is necessarily dependent on the bandgap presence and relatively weekly depends on SOC. To illustrate the result, let us turn to Fig. 5 where we display the electron density distribution in the reciprocal space after a strong chiral optical pulse whose waveform is shown in the inset. For the native (gapless) graphene, as Fig. 5 (a) shows, there is strictly no chirality or valley polarization: the distributions in both the K and K' valleys are mirror-symmetric with respect to a reflection in the y axis. As the bandgap increases, the K valley becomes progressively greater than that of the K' valley [panels (b) to (d)]. This is the effect of the topological resonance whose other signature is that the distribution of the electrons excited into the conduction band is narrowly concentrated around a closed curve caused the separatrix that separates the Bloch trajectories that encircle or not encircle the corresponding K point. The topological resonance effect allows one to induce a strong and lasting chiral memory in the hexagonal two-dimensional solid by just a single cycle of the chiral optical field.

We theoretically study the interaction of ultrashort optical pulses with gapped graphene. Such a strong pulse results in a finite conduction band population and a corresponding electric current, both during and after the pulse. Since gapped graphene has broken inversion symmetry, it has an axial symmetry about the *y* -axis but not about the *x*-axis. We show that, in this case, if the linear pulse is polarized along the *x*-axis, the rectified electric current is generated in the *y* direction. At the same time, the conduction band population distribution in the reciprocal space is symmetric about the *x*-axis. Thus, the rectified current in gapped graphene has an interband origin, while the intraband contribution to the rectified current is zero.

We theoretically study the strong-field absorption of an ultrafast optical pulse by a gapped graphene monolayer. At low field amplitudes, the absorbance in pristine graphene is equal to the universal value of 2.3 percent. Although the ultrafast optical absorption for low field amplitudes is independent of the polarization, linear or circular, of the applied optical pulse, for high field amplitudes, the absorption strongly depends on the pulse polarization. For a linearly polarized pulse, the optical absorbance is saturated at the value of approximately 1.4 percent for the pulse's amplitude of greater than 0.4 V/Å, but no such saturation is observed for a circularly polarized pulse. For the gapped graphene, the absorption of a linearly polarized pulse shows a weak dependence on the bandgap, while for a circularly polarized pulse, the absorption is very sensitive to the bandgap.

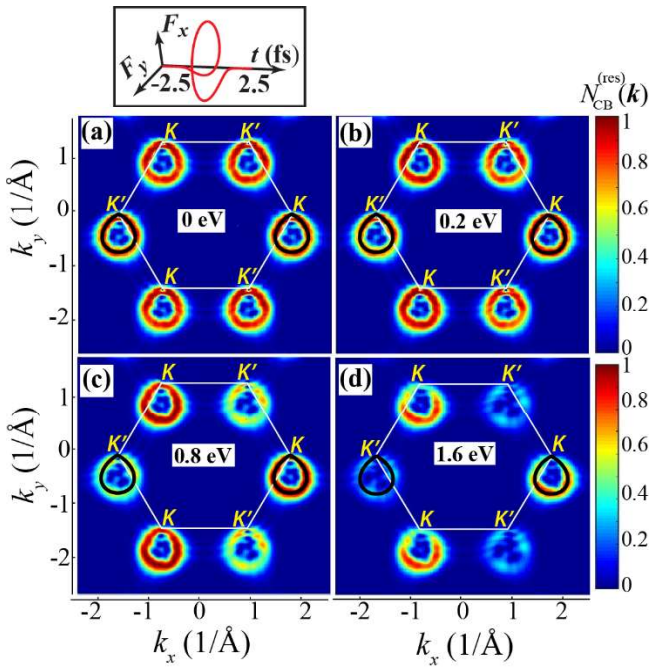

Fig. 5. Effect of topological resonance. We display residual CB population $N_{\mathrm{CB}}^{(\mathrm{res})}(\mathbf{k})$ for gapped graphene with variable bandgap in the extended zone picture. The applied optical pulse is right-hand circularly polarized with an amplitude of $F_0 = 0.5\,\mathrm{V}\text{Å}^{-1}$. Inset: Waveform of this pulse $\mathbf{F}(t) = \{F_x(t), F_y(t)\}$. as a function of time t. The white solid line shows the boundary of the first Brillouin zone with the K, K'-points indicated. The bandgap is 0 (a), 0.2 eV (b), 0.8 eV (c), and 1.6 eV (c), as indicated on the corresponding panels. The separatrix is shown in all panels with dash white line and solid black line for K and K' valleys respectively.

Finally, we theoretically introduce a topological spaser, which consists of a hexagonal array of plasmonic metal nanoshells containing an achiral gain medium in their cores. Such a spaser can generate two mutually time-reversed chiral surface plasmon modes in the K and K' valleys, which carry the opposite topological charges, ±1, and are described by a two-dimensional E'' representation of the D_{3h} point symmetry group. Due to the mode competition, this spaser exhibits a bistability: only one of these two modes generates, which is a spontaneous symmetry breaking. Such a spaser can be used for an

ultrafast all-optical memory and information processing, and biomedical detection and sensing with chirality resolution.

1.4 Applications of intense light to solids

1.4.1 Multi-electron Dynamics (Corkum)

Collision physics, wherein the fate of a colliding electron is mapped from an incident beam to a scattered beam, has been central to studying multi-electron dynamics for decades. A colliding electron may be deflected elastically or create new particles inelastically. Attosecond science, through its precise temporal control of ionization and recombination, can probe both possibilities while contributing the highly developed diagnostic tools of optics to collision physics.

Attosecond science's first attempt at probing multielectron dynamics used time-resolved photoelectron spectroscopy with well-characterized attosecond pulses. The relative time delay was measured for the emission of electrons from different orbitals in atoms or different bands in solids. However, in conventional attosecond science, it is difficult to separate time delay due to multielectron dynamics from time delay due to the electrostatic structure of system (how the electron interacts with its charged, but static environment) since both contribute to photoelectron time delay. To differentiate these effects, we have shown that one must turn to in-situ attosecond measurement.

In-situ methods were introduced as an efficient, all-optical approach to attosecond pulse measurement in which measurement and pulse generation take place simultaneously. However, in-situ measurement is insensitive to the phase of the transition moment. Therefore, the transition moment phase must be known for a complete pulse measurement.

However, this incomplete pulse measurement is a complete measurement of multi-electron dynamics. The re-collision electron must share its energy with the other parts of the many-electron system in any multi-electron response. Therefore, for in-situ measurement, any deviation from a hydrogen-like atto-chirp is a signature of multi-electron dynamics.

Experimentally, as described below, we observe multielectron dynamics associated with the giant plasmon resonance in Xenon. We observe multielectron dynamics in other systems as well.

Theoretically, also described below, we observe both the giant plasmon resonance in C60 and in Fano resonances in 1D Helium.

1.4.2 Single Image In-Situ Measurement

We have developed a single image measurement approach that generalizes in-situ measurement to a level where it is possible with a milli-Joule, λ=800 nm driver, to make one measurement per laser shot. The energy is used efficiently because we image the beam in the near field of the emitting medium, allowing this method of measurement to be extended well into the soft X-ray region. Figure 6 is a schematic of the measurement method.

We irradiate Xenon simultaneously by a carrier-envelope-phase (CEP) stabilized, few-cycle, polarization-gated pulse together with a much weaker CEP stabilized beam at a small angle, as seen in Figure 6. Together, these two fundamental beams create a grating and we measure this grating at each frequency of the attosecond pulse emission in the near field as seen in Figure 7 (a). The modulation on the dipole emission is clearly pronounced. It is used to determine the spectrum and spectral phase of the generated radiation. In Figure 7 (b) we see these parameters as measured between 20 and 55 eV. In Figure 7 (a)we extend the measurement up to 110 eV where we see the spectral signature of the giant plasmon resonance near 80 eV and the group delay of the beam in each spectral region, making a clear departure from its smoothly varying phase in this spectral region.

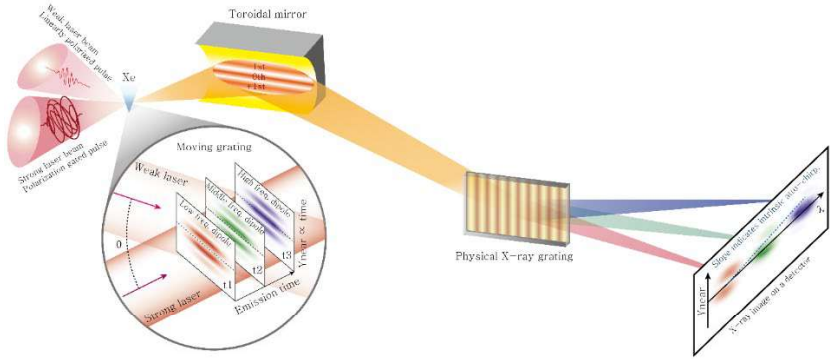

Fig. 6. A sketch of the experimental apparatus for single image measurement. The intense beam creates the attosecond pulse and the weaker beam, irradiation at an angle modulates the incident light. The spectrally resolved emission is imaged and measured.

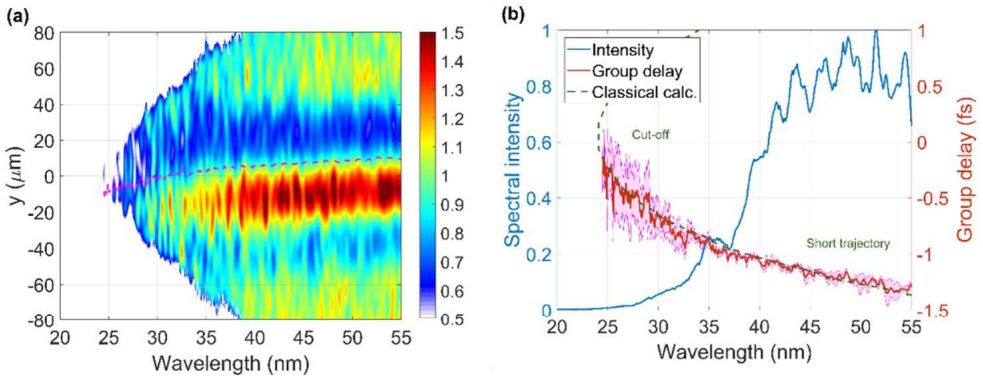

Fig. 7. (a) Shows the normalized difference between a beam created with and without a perturbing beam. (b) shows the spectrum and group delay measured for the attosecond beam within the spectral region of 25-55 eV.

1.4.3 The giant plasmon resonance in Xenon and C60 (Corkum)

To test the general concept, we turn to TD-DF simulations. We simulate C60, a somewhat similar system to Xenon, due to its computational accessibility. To keep the dimensionality of the simulation tractable, we simulate a linearly polarized 25 fs, 800 nm pulse with intensity 2×10^{13} W cm^{-2} and a co-propagating perturbing second-harmonic beam field with $2\text{x}10^{-9}$ W cm^{-2}. We reduce the dimensionality of the simulation further by approximating C_{60} as a closed-shell spherical jellium shell. The results of this simulation are shown in Figure 8 (right). The shaded blue curve is

the group delay of an attosecond pulse generated directly calculated from the simulation. The black circles depict the reconstructed times of emission of the attosecond pulse spectra from the simulated collinear in situ measurement. The qualitative agreement between experiment and theory for these similar systems shows that the excitation of the plasmonic resonance occurs during propagation and lies within the domain of in-situ techniques.

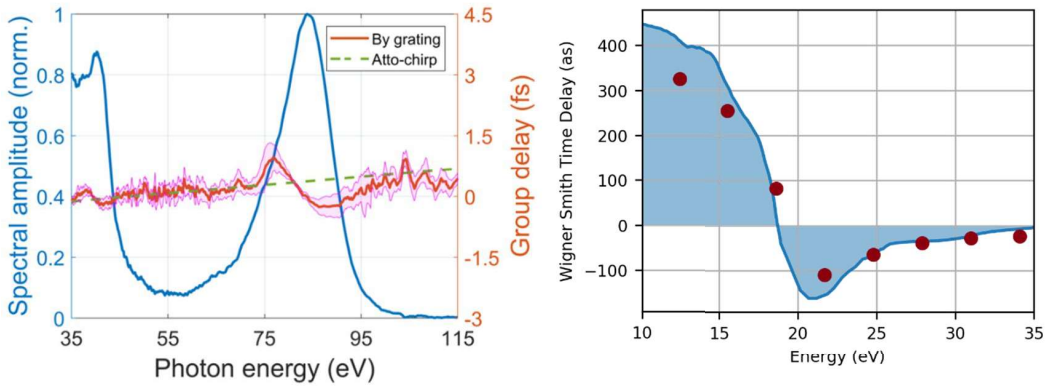

Fig. 8. Left: Experimental measurement showing the Giant Plasmon resonance through the spectral amplitude (left axis) and group delay (right axis). The standard deviation of a set of 20 measurements is shown by the pink shaded area. Right: The blue shaded area shows the Wigner Smith time delay calculated using time dependent density functional theory. The red data points are a simulation of a two-color in-situ measurement.

1.4.4 High harmonics from solids (Corkum)

MgO is an important medium for generating high harmonics from solids extending to 25 eV. We have studied how to produce harmonics efficiently from MgO and we have applied a second new measurement method to determine the structure of the radiation that is created. While this work was not complete by the end of the MURI 9 grant, it is clear that radiation created by Block oscillations can be differentiated from radiation created by re-collision, opening a path to study each of them individually.

2. List of Submissions or Publications during the Current Reporting Period (Peer and Non-Peer Reviewed Journals)

[1] Seunghwoi Han, Jie Li, Zheyuan Zhu, Andrew Chew, Esben W. Larsen, Yi Wu, Shuo Sean Pang, and Zenghu Chang, "Tabletop Attosecond X-rays in the Water Window," Advances in Atomic, Molecular, and Optical Physics **69**, ISBN10:0128209879 (2020).

[2] Jie Li, Jian Lu, Andrew Chew, Seunghwoi Han, Jialin Li, Yi Wu, He Wang, Shambhu Ghimire, Zenghu Chang, "Attosecond Science based on High Harmonic Generation from Gases and Solids," Nature Communications **11**, 2748 (2020). https://doi.org/10.1038/s41467-020-16480-6

[3] Yi Wu, Fangjie Zhou, Esben W. Larsen, Fengjiang Zhuang, Yanchun Yin, and Zenghu Chang,

"Generation of few-cycle multi-millijoule 2.5 μm pulses from a single-stage Cr^{2+}:ZnSe amplifier," Scientific Reports **10**, 7775 (2020).
https://doi.org/10.1038/s41598-020-64330-8

[4] Jialin Li, Yang Wang, Tianyi Guo, Jonathon White, Matthew Weidman, Yi Wu, Kai Hu, Marieke F Jager, Christopher J Kaplan, Romain Geneaux, Daniel M Neumark, Stephen R Leone, Graham G Brown, Paul Corkum, and Zenghu Chang, "Beam optimization in a 25 TW femtosecond laser system for high harmonic generation," J. Phys. B: At. Mol. Opt. Phys. **53,** 145602 (2020).
https://doi.org/10.1088/1361-6455/ab8e57

[5] Zheyuan Zhu, Johnathon White, Zenghu Chang and Shuo Pang, "Attosecond pulse retrieval from noisy streaking traces with conditional variational generative network," Scientific Reports 43583 (2020).
https://doi.org/10.1038/s41598-020-62291-6

[6] Zheyuan Zhu, Yangyang Sun, Johnathon White, Zenghu Chang and Shuo Pang, "Signal retrieval with measurement system knowledge using variational generative model," IEEE Access **8**, 47963 – 47972 (2020).
DOI: 10.1109/ACCESS.2020.2978435

[7] Jie Li, Andrew Chew, Shuyuan Hu, Jonathon White, Xiaoming Ren, Seunghwoi Han, Yanchun Yin, Yang Wang, Yi Wu, and Zenghu Chang, "Double optical gating for generating high flux isolated attosecond pulses in the soft x-ray regime," Optics Express **27**, 30280-30286 (2019).
https://doi.org/10.1364/OE.27.030280

[8] Zenghu Chang, "Enhancing keV high harmonic signals generated by long-wave infrared lasers," OSA Continuum **2**, 2131-2136 (2019).
https://doi.org/10.1364/OSAC.2.002131

[9] Nariyuki Saito, Hiroki Sannohe, Nobuhisa Ishii, Teruto Kanai, Nobuhiro Kosugi, Yi Wu, Andrew Chew, Seunghwoi Han, Zenghu Chang, and Jiro Itatani, "Real-time observation of electronic, vibrational, and rotational dynamics in nitric oxide with attosecond soft X-ray pulses," Optica **6**, 1542 (2019).
https://doi.org/10.1364/OPTICA.6.001542

[10] R. Geneaux, H. J. B. Marroux, A. Guggenmos, D. M. Neumark, and S. R. Leone, "Transient absorption spectroscopy using high harmonic generation: a review of ultrafast X-ray dynamics in molecules and solids," Phil. Trans. R. Soc. A **377**, 2145 (2019).
DOI: 10.1098/rsta.2017.0463

[11] S. K. Cushing, A. Lee, I. J. Porter, L. M. Carneiro, H.-T. Chang, M. Zürch, and S. R. Leone, "Differentiating photoexcited carrier and phonon dynamics in the Δ, L, and Γ valleys of Si(100) with transient extreme ultraviolet spectroscopy," J. Phys. Chem. C **123**, 3343 (2019).
DOI: 10.1021/acs.jpcc.8b10887

[12] C. J. Kaplan, P. M. Kraus, E. M. Gullikson, L. J. Borja, S. K. Cushing, M. Zürch, H.-T. Chang, D. M. Neumark, and S. R. Leone, "Retrieval of the complex-valued refractive index of germanium near the $M_{4,5}$ absorption edge," J. Opt. Soc. Am. B **36**, 1716 (2019).
DOI: 10.1364/JOSAB.36.001716

[13] S. K. Cushing, I. J. Porter, B. R. de Roulet, A. Lee, B. M. Marsh, S. Szoke, M. E. Vaida, and S. R. Leone, "Layer-resolved ultrafast extreme ultraviolet measurements of hole transport in a Ni-TiO_2-Si photoanode," Sci. Adv. **6**, eaay6650 (2020).
DOI: 10.1126/sciadv.aay6650

[14] B. A. Erickson, Z. N. Heim, E. Pieri, E. Liu, T. J. Martinez, and D. M. Neumark, "Relaxation dynamics of hydrated thymine, thymidine, and thymidine monophosphate probed by liquid jet time-resolved photoelectron spectroscopy," J. Phys. Chem A. **123**, 10676 (2019).
https://doi.org/10.1021/acs.jpca.9b08258

[15] A. Camper, Hyunwook Park, S. J. Hageman, G. Smith, T. Auguste, P. Agostini and L. F. DiMauro, "High relative-phase precision beam duplicator for mid-infrared femtosecond pulses" Opt. Lett. **44**, 5465 (2019).
https://doi.org/10.1364/OL.44.005465

[16] A. Krobenko, T. J. Hammond, C. Zhang, A. Yu. Naumov, D. M. Villeneuve, and P. B. Corkum, "High-harmonic generation in solids driven by counter-propagating pulses," Opt. Express. **27**, 32630 (2019).
https://doi.org/10.1364/OE.27.032630

[17] D. H. Ko, G. G. Brown, C. Zhang and P. B. Corkum, "Delay measurement of attosecond emission in solids", J. Phys B. **53**, 124001 (2020).
https://doi.org/10.1088/1361-6455/ab81e7

[18] G. Brown, D.H. Ko, C. Zhang and P.B. Corkum, manuscript in preparation.

[19] D. H. Ko, G. G. Brown, C Zhang and P. B. Corkum, manuscript on using CEP dependence of the attosecond cut-off for measurement in preparation.

[20] D. H. Ko, G. G. Brown, C Zhang and P. B. Corkum, manuscript on single image measurement in preparation.

[21] S. Sederberg, F. Kong, P. B. Corkum, "Tesla-Scale Terahertz Magnetic Impulses", Phys. Rev. X **10**, 011063 (2020).
https://doi.org/10.1103/PhysRevX.10.011063

[22] S. A. Oliaei Motlagh, F. Nematollahi, V. Apalkov, and M. I. Stockman, "Topological Resonance and Single-Optical-Cycle Valley Polarization in Gapped Graphene," Phys. Rev. B **100**, 115431-1-10 (2019).
https://doi.org/10.1103/PhysRevB.100.115431

[23] S. A. Oliaei Motlagh, F. Nematollahi, A. Mitra, A. J. Zafar, V. Apalkov, and M. I. Stockman, "Ultrafast Optical Currents in Gapped Graphene," Journal of Physics: Condensed Matter **32**, 065305-1-8 (2019). https://doi.org/10.1088/1361-648X/ab4fc7

[24] S. A. O. Motlagh, A. J. Zafar, A. Mitra, V. Apalkov, and M. I. Stockman, "Ultrafast Strong-Field Absorption in Gapped Graphene," Phys. Rev. B **101**, 165433-1-7 (2020). https://doi.org/10.1103/PhysRevB.101.165433

[25] J.-S. Wu, V. Apalkov, and M. I. Stockman, "Topological Spaser," Phys. Rev. Lett. **124**, 017701-1-5 (2020). https://doi.org/10.1103/PhysRevLett.124.017701

3. List of Presentations Given During the Current Reporting Period

[1] Zenghu Chang, "Attosecond X-rays in the Water Window," International OSA Network of Students (IONS) and the Optics, Photonics & Upcoming Methods and Applications (OPUMA), June 8 – 12, 2020. Online.

[2] Zenghu Chang, "Attosecond transient absorption spectroscopy at nitrogen K edge," 2019 Joint AFORS-ARO Attosecond MURI Review, Nov. 21-22, 2019, Arlington, VA.

[3] Zenghu Chang, "High power MIR lasers for generating attosecond water window X-rays," 2019 Joint AFORS-ARO Attosecond MURI Review, Nov. 21-22, 2019, Arlington, VA.

[4] Zenghu Chang, (Physics colloquium), "Attosecond X-rays Reached the Water Window," The University of Georgia. September 5, 2019. Athens, Georgia.

[5] Zenghu Chang, (plenary), "Frontier of attosecond source development and applications," Frontier Science and Applications of Attosecond Light Source. Aug. 21-22, 2019. Beijing, China.

[6] Zenghu Chang, "Novel high power infrared lasers for attosecond science," The 12th International Symposium on Photonics and Optoelectronic. Aug. 17-19, 2019. Xi'an, China.

[7] Zenghu Chang, "Attochirp compensation and characterization beyond C K-edge," 7th International Conference on Attosecond Science and technology, July 1-5, 2019. Szeged, Hungary.

[8] Zenghu Chang, "Novel mid-infrared lasers for pushing the attosecond science frontier," 21st Photonics North Conference, May 21-23, 2019. Quebec city, Canada.

[9] Zenghu Chang, "Novel high power infrared lasers for strong field science," Directed Energy Science & Technology Symposium, April 8-12, 2019. Destin, FL.

[10] Zenghu Chang, “Institute for the Frontier of Attosecond Science and Technology (iFAST),” Mini-Workshop on Attosecond Physics, University of Central Florida. April 2, 2019.

[11] Zenghu Chang (online lecture OPT392), “Attosecond Optics,” University of Rochester, April 1, 2019.

[12] Zenghu Chang (colloquium), “Approaching the Attosecond keV X-ray Frontier,” Department of Physics, Missouri Science & Technology. March 7, 2019.

[13] S. R. Leone, (invited) “Attosecond Probing of Solid-State Dynamics,” Physics and Astronomy Colloquium, The University of Georgia, Athens, GA, January 2019.

[14] S. R. Leone, (invited) “Ultrafast X-Ray Molecular Dynamics,” Applied Physics Seminar, The University of Georgia, Athens, GA, January 2019.

[15] S. R. Leone, (invited) “Attosecond Electron Dynamics: From Atoms to Semiconductor Solids,” Dreyfus Foundation Lecture, The State University of New York (SUNY), Geneseo, NY, March 2019.

[16] S. R. Leone, (invited) “Ultrafast X-Ray Molecular Dynamics,” Gislason Lecture, University of Illinois, Chicago, Chicago, IL, March 2019.

[17] S. R. Leone, (invited) “Attosecond Probing of Solid-State Dynamics,” Gislason Lecture, University of Illinois, Chicago, Chicago, IL, March 2019.

[18] S. R. Leone, (invited) “Attosecond Electron Dynamics in Solids,” The Brian Bent Lecturer, Columbia University, New York, NY, April 2019.

[19] S. R. Leone, (invited) “Attosecond Electron Dynamics: From Atoms to Semiconductor Solids,” Chemical Sciences & Engineering Colloquium, Argonne National Laboratories, Argonne, IL, April 2019.

[20] S. R. Leone, (invited) “Attosecond Electron Dynamics in Solids,” Physical Chemistry Colloquium, University of California at San Diego, San Diego, CA, May 2019.

[21] S. R. Leone, (invited) “An Attosecond X-Ray Revolution in Solid-State Dynamics,” ICFO School on Frontiers in Attosecond Science Invited Lecturer, The Institute of Photonic Sciences, Barcelona, Spain, July 2019.

[22] S. R. Leone, (invited) “Attosecond Electron Dynamics in Solids,” ICFO School on Frontiers in Attosecond Science Seminar Series, The Institute of Photonic Sciences, Barcelona, Spain, July 2019.

[23] S. R. Leone, (invited) “Attosecond Probing of Atomic and Solid-State Dynamics,” Quantum Lecture Seminar Series, Louisiana State University, Baton Rouge, LA, February 2020.

[24] S. R. Leone, (invited) “Ultrafast X-Ray Molecular Dynamics,” Quantum Lecture Seminar Series, Louisiana State University, Baton Rouge, LA, February 2020.

[25] D. M. Neumark, (invited) "Solvation dynamics in clusters and liquid jets," Ruhr University, Bochem, Germany, Sept. 2018.

[26] D. M. Neumark, (invited) "Time-resolved dynamics in gas-phase clusters and liquid jets," Molecular and Ionic Clusters Gordon Research Conference, Ventura, CA, January, 2020.

[27] D. M. Neumark, (invited) "Time-resolved dynamics in gas-phase clusters and liquid jets," S3C Conference, Davos, Switzerland, Feb. 2020.

[28] L. F. DiMauro, “Wavelength scaling of strong field physics”, IBS, Gwangju, Korea, invited talk, August, 2019.

[29] P. B. Corkum, “High harmonic generation with structured light beams,” PQE 2019, Snowbird, Utah, USA, Plenary, 9 JAN, 2019.

[30] P. B. Corkum, “A Plasma Perspective on Attosecond Science in Solids and Gases,” University of Maryland Physics Colloquium, College Park, MD, USA, Colloquium, 19 FEB, 2019.

[31] P. B. Corkum, “Attosecond pulses generated in gases and solids,” University of Connecticut, Storrs, CT, USA, Pollack Lecture, 12 APR, 2019.

[32] P. B. Corkum, “Vector beams, high harmonic generation and THz solenoidal magnetic fields,” Universitat Bonn, Bonn Germany, Invited Talk, 30 APR, 2019.

[33] P. B. Corkum, U“Extending our time horizon to attoseconds and beyond,” niversitat Bonn, Bonn, Germany, Wolfgang-Paul Lecture, 2 MAY, 2019.

[34] P. B. Corkum, “Extending the Scientific Time Horizon to Attoseconds,” 2019 Humboldt Kolleg, Ottawa, ON, Canada, Plenary, 10 MAY, 2019.

[35] P. B. Corkum, “Extending the Scientific Time Horizon to Attoseconds,” IOP Newton Lecture, London, UK, Newton Lecture, 13 MAY, 2019.

[36] P. B. Corkum, “Vector beams, high harmonic generation and THz solenoidal magnetic fields,” Physics Seminar, University of British Columbia, Vancouver, BC, Canada, Invited Talk, 17 MAY, 2019.

[37] P. B. Corkum, “Attosecond pulses generated in gases and solids,” Special Symposium in AMO, Sinica IAMS, Taipei, Taiwan, Tutorial, 21 MAY, 2019.

[38] P. B. Corkum, “A molecule takes a selfie while creating the world’s shortest pulses,” Top Honorary Lecture, National Cheng Kung University, Tainan, Taiwan, Public Lecture, 23 MAY, 2019.

[39] P. B. Corkum, "Vector beams, high harmonic generation and sub-focal spot coherent control," CAP Symposium, Simon Fraser University, Vancouver, BC, Invited Talk, 4 JUN, 2019.

[40] P. B. Corkum, "High harmonic generation with structured light beams," Frontiers in Nonlinear Physics Boat Conference, Russia, Plenary, 28 JUN, 2019.

[41] P. B. Corkum, "High harmonic generation with structured light beams," OSA Nonlinear Optics Topical Meeting, Waikoloa Beach, Hawaii, USA, Plenary, 17 JUL, 2019.

[42] P. B. Corkum, "Vector Beams, High Harmonic Generation and THz Solenoidal Magnetic Fields," Gordon Research Conference, Salve Regina University, Newport, RI, USA, Invited Talk, 14 AUG, 2019.

[43] P. B. Corkum, "Using light to control electrons that, in turn, create new light sources," Otto Stern Fest, Universität Frankfurt, Frankfurt, Germany, Keynote, 3 SEP, 2019.

[44] P. B. Corkum, "A molecule takes a selfie while creating the world's shortest light pulses," Ta-You Wu Lecture, State University of New York at Buffalo, Buffalo, USA Public Lecture, 25 OCT, 2019.

[45] P. B. Corkum, "Functional Dynamics – visualizing molecules in action," Nature Conference, Arizona State University, Tempe, AZ, USA, Plenary, 7 NOV, 2019.

4. Honors and Awards Received During the Current Reporting Period

Louis DiMauro, 2017 APS Arthur Schawlow Prize in Laser Science.

Zenghu Chang, UCF College Excellence in Research Award, 2020.

Zenghu Chang, UCF Research Incentive Award, 2020.

Paul Corkum, Royal Medal from the Royal Society, London, UK, for his major contributions to laser physics and the development of the field of attosecond science.

Paul Corkum, Schneider Medal, National Research Council Canada, Ottawa, Canada, (their highest distinction bestowed upon employees).

Stephen Leone, 2019 Distinguished Dreyfus Foundation Lectureship, The State University of New York (SUNY)

Stephen Leone, 2019 Distinguished Gislason Lectureship, University of Illinois, Chicago

Stephen Leone, 2019 Distinguished Brian Bent Lectureship, Columbian University

5. Patents Awarded During the Current Reporting Period

Z. Chang *et al*., The U.S. Provisional Application Serial Number 16/032,808.
K. Murari *et al*., The U.S. Provisional Application Serial Number 62/768,643.

6. Students / Postdocs, Supported Personnel Metrics During the Current Reporting Period (Name, % Supported, and Total for Each Category: Grad, Postdoc, Faculty, Undergrad, Etc.)

6.1 Graduate Students

UCB, Hung-Tzu Chang (50%)
UCB, Christopher J. Kaplan (50%)
UCB, Holly Williams (50%)
UCB, Blake Erickson (50%)
OSU, Stephen Hageman, 100%
OSU, Greg Smith, 100%
UCF, Fangjie Zhou, 70%
UCF, Zheyuan Zhu, 44%
UCF, Graham Brown, 100%
UCF, Jonathon White, 100%
UCF, Zachary Alphonse Marra, 87.5%
GSU, Fatemeh Nematollahi, 100%

6.2 Faculty

Zenghu Chang, 1.5 summer month.
Stephen Leone, none
Daniel Neumark, 7 days in summer.
Vadym Apalkov, 3 summer months.
Mark Stockman, 1 summer month.
Louis DiMauro, 1 summer month.

6.3 Post Doctoral Scholar

UCB, Romain Géneaux (100%)
UCF, Matthew Weidman, 100%
UCF, Jialin Li, 85%
UCF, Seunghwoi, 87.8%
UCF, Yi Wu, 55.4%
GSU, S. A. O. Motlagh, 100%
GSU, Jhih-Sheng Wu, 100%
OSU, Li Fang, 30%
OSU, Zhou Wang, 60%

6.4 Administrative

Kathleen Buckley (8%)
Michelle Haskins 8%

7. Graduating Metrics

Jie Li received a PhD degree in May 2018.
Shuyuan Hu received an MSc degree in May 2018.
Christopher Kaplan received a PhD degree in May 2019.
Andrew Chew received a PhD degree in July 2020.

8. Technology Transfer

None.